Supplement of Atmos. Chem. Phys., 26, 5879–5899, 2026
https://doi.org/10.5194/acp-26-5879-2026-supplement

Atmospheric Chemistry and Physics
Open Access
EGU

Supplement of

A combined observational and modelling approach to evaluate aerosol–cirrus interactions at high and mid-latitudes

Elena De La Torre Castro et al.

Correspondence to: Elena De La Torre Castro (elena.delatorrecastro@dlr.de)

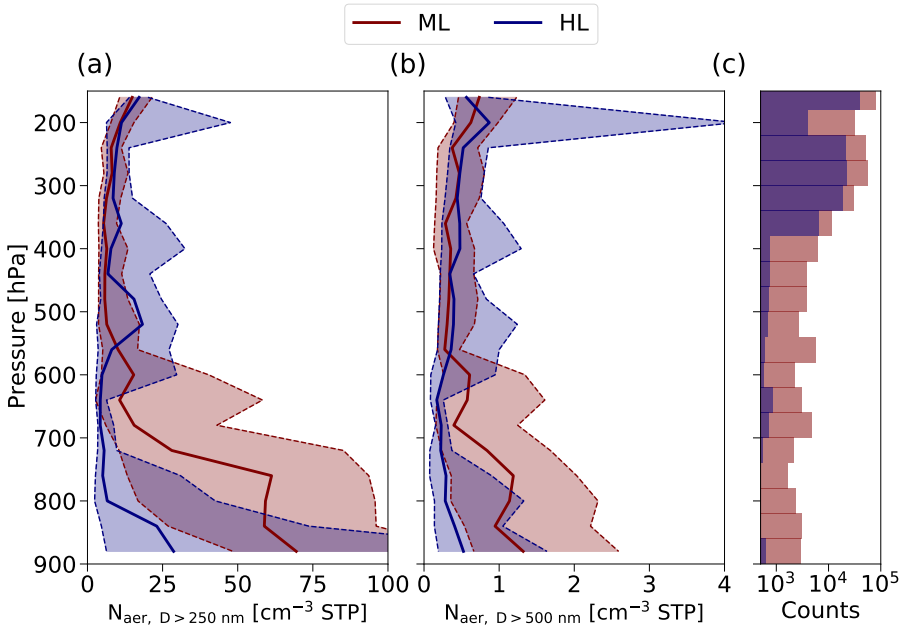

Figure S1. Same as Fig. 1 but comparing the particle size ranges (a) $D > 250$ nm and (b) $D > 500$ nm from the OPC measurements. Median profiles are indicated with solid lines, the areas between the 25^{th} and 75^{th} percentiles are filled and indicated within dashed lines. (c) Number of observations per pressure bin of 40 hPa each.

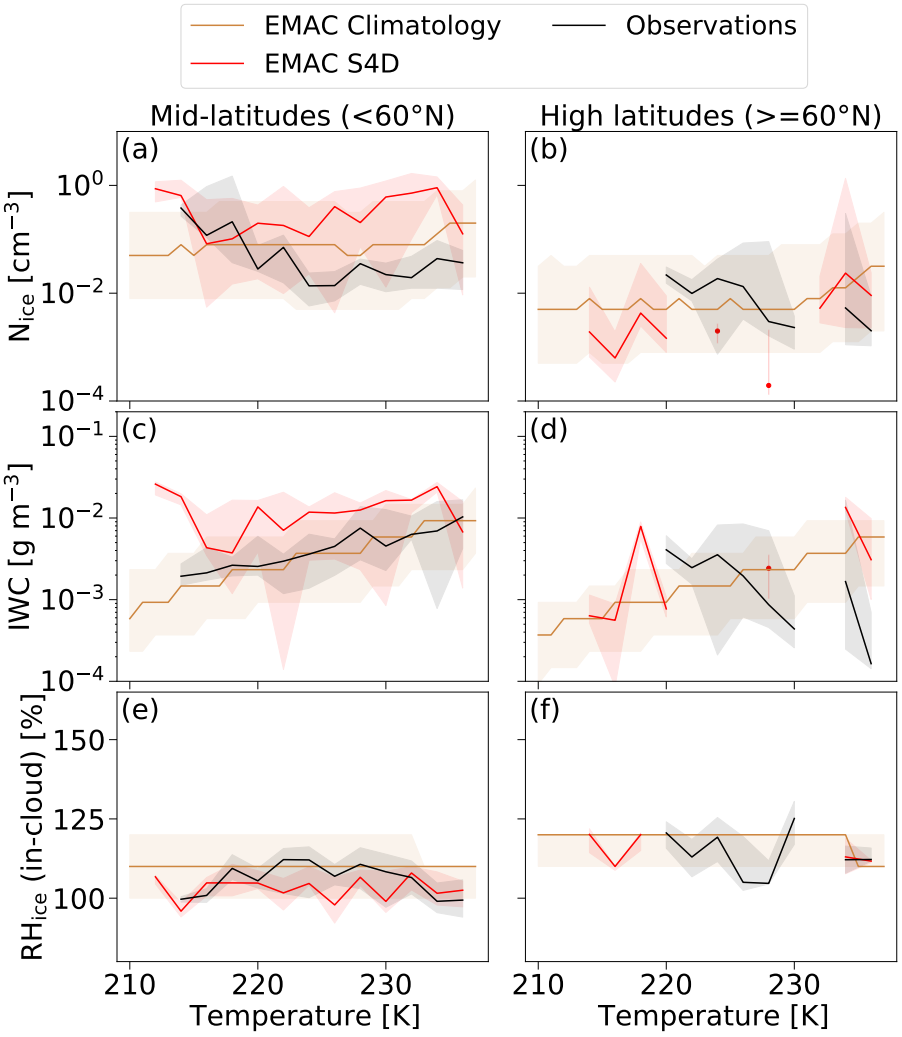

Figure S2. As in Fig. 5, but without the all-data panels and with a model climatological average (brown) for June-July 2014-2021 included as reference. Climatological model output was not obtained applying the diagnostic submodel S4D (Sampling in 4 Dimensions; Jöckel et al. 2010) along the flight tracks, but instead by averaging over the latitude, longitude and altitude range of the CIRRUS-HL flights.

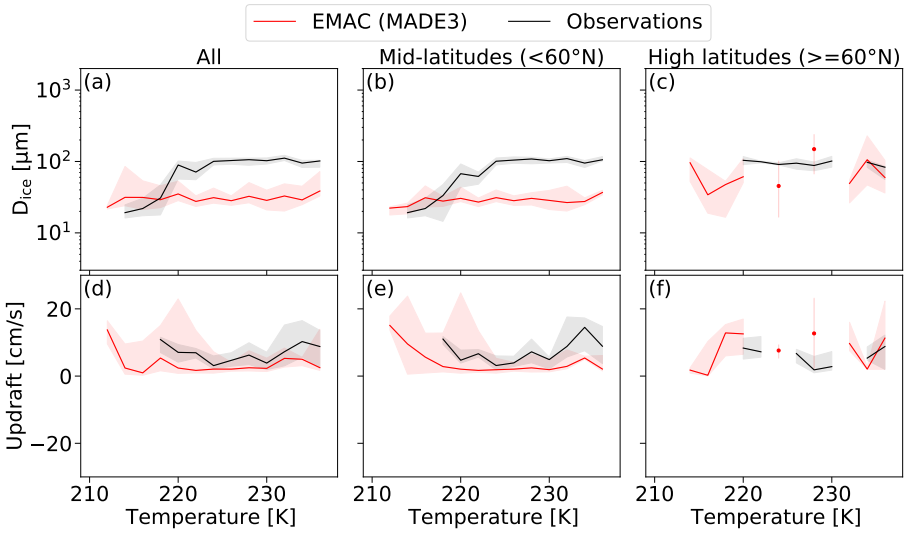

Figure S3. Comparison of temperature profiles of microphysical properties of ice clouds between the observations (black) and the EMAC model (red) during the CIRRUS-HL campaign (as in Fig. 5): (a), (b), and (c) mean volume diameter (D_{ice}); (d), (e), and (f) updraft velocity. Note that the ice crystal mean volume diameter in the model is not an independent quantity as it is calculated from the simulated IWC values, assuming spherical particles. The left column (a, d) represent all data, while the center (b, e) and right column (c, f) show only mid- and high-latitude data points, respectively. Solid lines indicate median values per 2 K temperature bin and shaded areas extend from 25^{th} and 75^{th} percentiles. Discontinuous lines appear in the high-latitude panels due to insufficient statistics in those temperature bins.

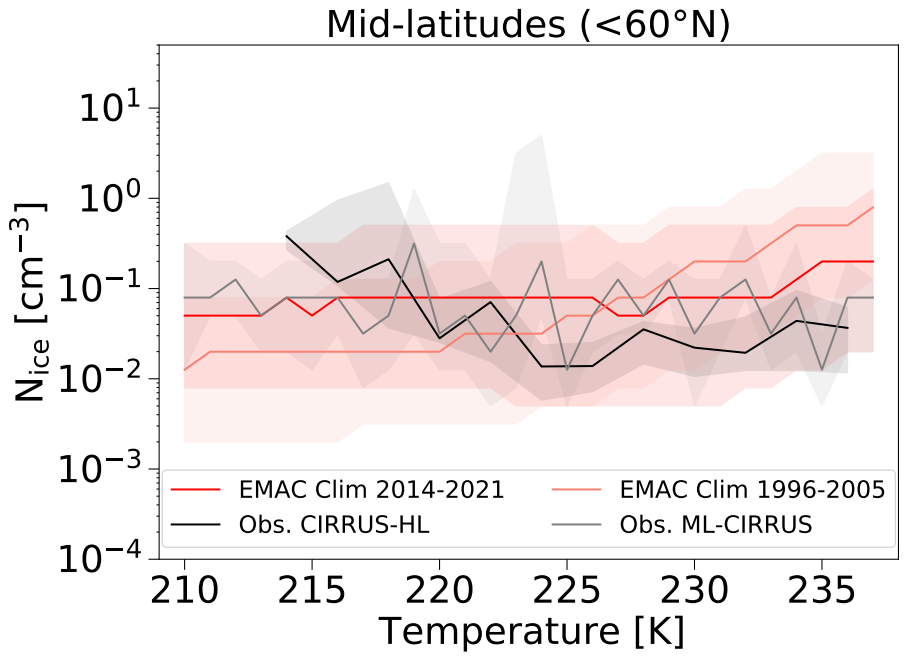

Figure S4. Similar as Fig. 5 (b) but comparing observations from CIRRUS-HL (black) and ML-CIRRUS (gray) with climatological model averages over the corresponding periods: 2014-2021 for CIRRUS-HL (red) and 1996-2005 for ML-CIRRUS (salmon). Observational and model data for ML-CIRRUS are taken from the study by Righi et al., (2020).

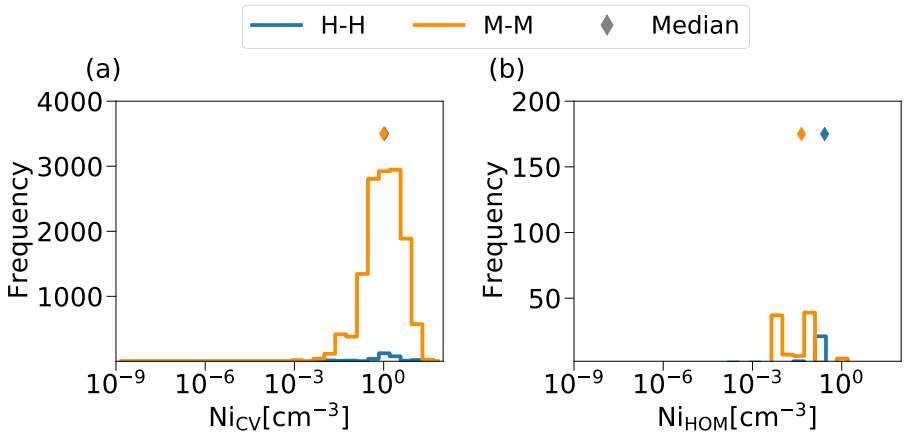

Figure S5. Absolute frequency distribution of newly formed ice crystals from (a) convection (CV), and (b) homogeneous freezing (HOM) along all backward trajectories of cirrus formed and measured at high latitudes (H-H, blue) and cirrus formed and measured at mid-latitudes (M-M). The model output has a time resolution of one hour over the period June-July 2021 to adjust to the backward trajectories time step.

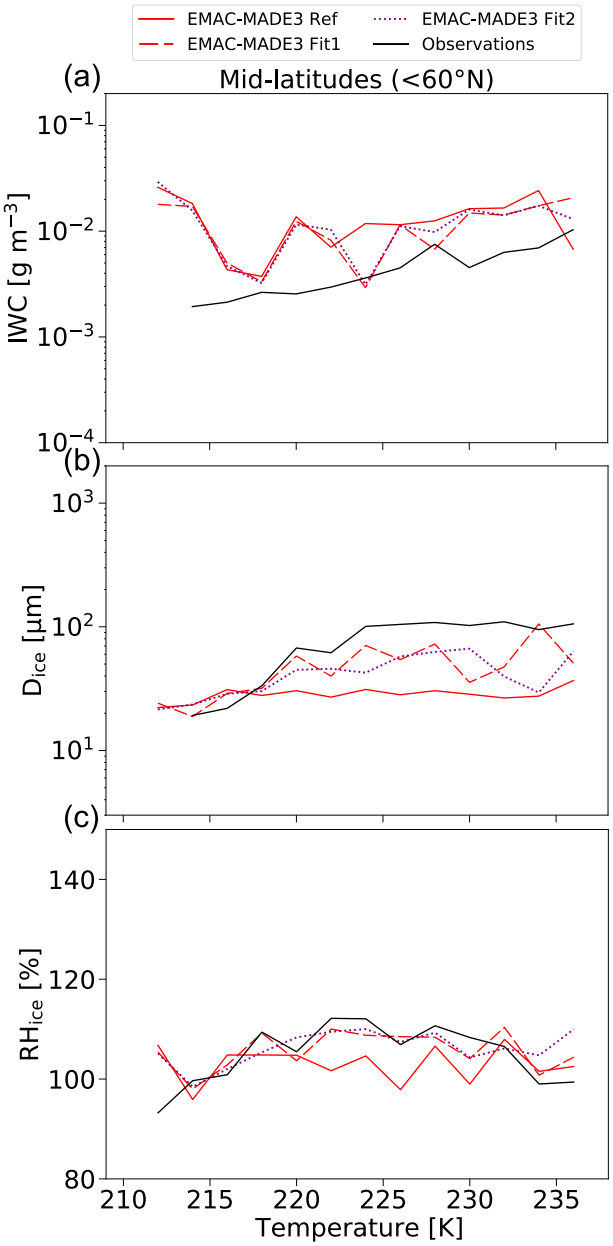

Figure S6. Comparison of observations and model at mid-latitudes for the reference case (ref, red solid line), fit1 (red dashed line), and fit2 (purple dotted line), as in Fig. 7. Shown are (a) ice water content (IWC), (b) mean volume diameter (D_{ice}), and (c) relative humidity over ice ($\mathrm{RH_{ice}}$). Note that the ice crystal mean volume diameter in the model is not an independent quantity as it is calculated from the simulated IWC values, assuming spherical particles.

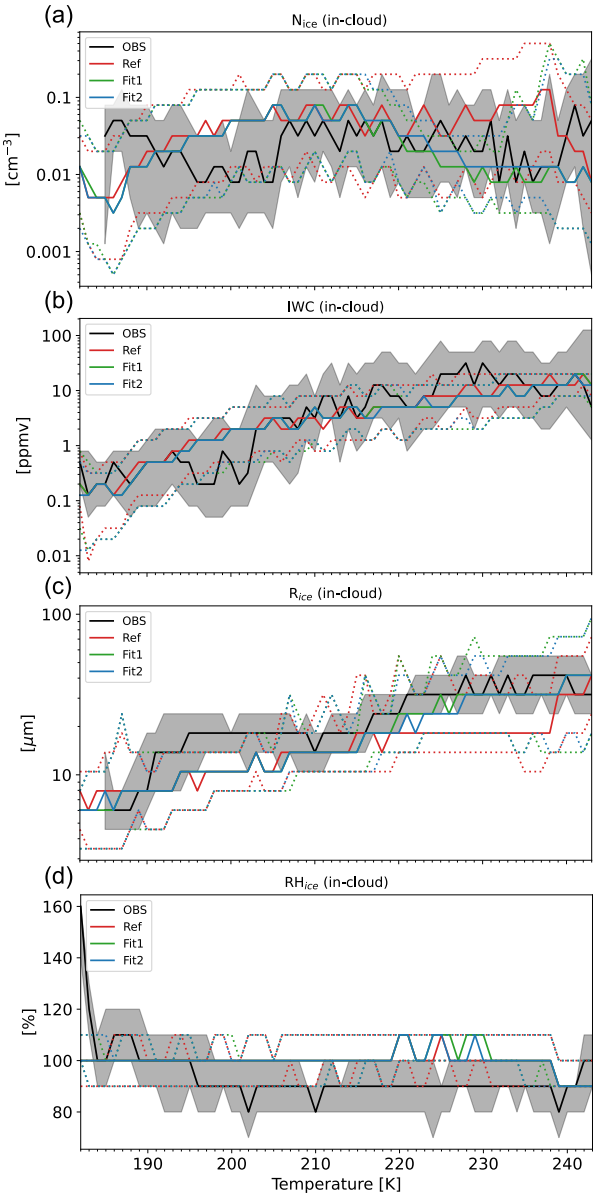

Figure S7. Comparison of simulated (a) in-cloud ice crystal number concentrations (N_{ice}), (b) ice water content (IWC), (c) ice particle radius (R_{ice}), (d) and in-cloud relative humidity over ice ($\mathrm{RH}_{\mathrm{ice}}$) from the cases Ref, Fit1, and Fit2 with an observational climatology derived from various flight campaigns (Krämer et al., 2016, 2020), considering the simulated period from 2014-2016. Solid lines show median values, shadings and dotted lines show the 25^{th} to 75^{th} percentile range.